Proceedings of the Korean Nuclear Society Autumn Meeting
Cheju, Korea, May 2001

New Calculation Method of the Solid Angle Subtended by a Circular Disk at a Point

Sungho Chang, Gyuseong Cho, Wanno Lee and *Woo Sung Hur

Korea Advanced Institute of Science and Technology
373-1 Kusong-dong, Yusong-gu, Taejon, 305-701 Korea

*Simuline, 3-1 Expo park, Doryong-dong, Yusong-gu, Taejon,

Abstract

New calculation method of the solid angle subtended by a circular disk at a point is presented. For verification of this method, the comparison with Gardner’s calculation solid angle subtended by a disk at a point lies on the axis of a disk and average solid angle subtended by a circular disk to a parallel coaxial disk is performed.

Introduction

Recently optical fibers have been used often as radiation detector itself or as photo collecting probe of the light emitted from various types of scintillation material. The geometrical efficiency is expressed as the solid angle divided by 4π. For the accurate estimation of the geometrical efficiency of an optical fiber detector, the accurate value of the solid angle is needed because the entrance area of the optical fiber is small and it has often a limited angle of acceptance.

Generally, when the refractive material is used as the detector window, a portion of incident light doesn’t enter into the detector because of the total reflection at the detector window surface. And it is necessary to consider the incident angle of light to an optical fiber in the calculation of the solid angle because the incident angle of light determines whether the optical fiber accepts light or not.

Several researchers have developed calculation methods for the solid angle subtended by a circular disk at a point source with approximation of equal-area square [1] and polygon [2,3] in Cartesian coordinate system. These methods can be applied to calculate the average solid angle subtended by a circular disk coaxial to another one. However, these methods can' t be applied to in the case when the detector accepts the light only for a certain angles because there is a limit with the angle of acceptance by detector.

New solid angle calculation method that can treat the incident angle of light by the use of the spherical polar coordinate system is proposed. It can be applied to where incident angle of light is important and it is easily extensible to the case of two parallel disks that are not coaxial.

Calculation and Results

In spherical coordinates, the differential solid angle is given as

$$d\Omega = \frac{dA}{r^2} = \sin\theta \; d\theta \; d\phi \qquad \text{Eq. 1}$$

Integrating of Eq. 1, the formula of solid angle is as follows

$$\Omega = \iint \sin\theta \; d\theta \; d\phi \qquad \text{Eq. 2}$$

Figure 1 shows a point source and a disk parallel to x-y plane and variables needed to calculate the solid angle between them. By using the notation in Figure 1, equation of circle in three dimension is

$$\begin{aligned} & x^2 + (y - V)^2 = R^2 \\ & z = H \end{aligned} \qquad \text{Eq. 3}$$

After conversion of x, y, z to spherical polar coordinate system, they are represented as follows.

$$\begin{aligned} & x = r \sin\theta \cos\phi \\ & y = r \sin\theta \sin\phi \\ & z = r \cos\theta \end{aligned} \qquad \text{Eq. 4}$$

Putting the Eq. 4 into the Eq. 3, a quadratic equation is acquired.

$$H^2 \tan^2\theta(\cos^2\varphi + \sin^2\varphi) - 2HV\tan\theta\sin\varphi + V^2 = R^2 \qquad \text{Eq. 5}$$

Solving the Eq. 5, about θ,

$$\theta = \tan^{-1}\frac{HV\sin\varphi \pm \sqrt{(HV)^2\sin^2\varphi - H^2(V^2 - R^2)}}{H^2} \qquad \text{Eq. 6}$$

Eq. 6 shows the azimuth angle determines the polar angle, and it is the key point of the this proposed method.

As shown in Figure 1, if V > R, integrating Eq. 2 over θ gives

$$\Omega(R,H,V) = \int_{\varphi 1}^{\varphi 2}(-\cos\theta_2 + \cos\theta_1)d\varphi \qquad \text{Eq. 7}$$

where

$$\theta_2 = \tan^{-1}\frac{HV\sin\varphi + \sqrt{(HV)^2\sin^2\varphi - H^2(V^2 - R^2)}}{H^2}$$
$$\theta_1 = \tan^{-1}\frac{HV\sin\varphi - \sqrt{(HV)^2\sin^2\varphi - H^2(V^2 - R^2)}}{H^2} \qquad \text{Eq. 8}$$

The interval of the φ is as follows

$$\cos^{-1}\frac{R}{V} \le \varphi \le \pi - \cos^{-1}\frac{R}{V} \qquad \text{Eq. 9}$$

As shown in Figure 2, if V < R, integrating Eq. 2 over θ gives

$$\Omega(R,H,V) = \int_{\varphi 1}^{\varphi 2}(-\cos\theta_2 - \cos\theta_1 + 2)d\varphi \quad , \qquad 0 \le \varphi \le \pi \qquad \text{Eq. 10}$$

The derived equations are applied to the case that a point source which lies on the axis of a disk and to the case of two parallel coaxial disks as shown in Figure 3. Their results are compared with the references for verification.

The formula of the first case given in ref. [1] is as follows

$$\Omega_p = 2p\left(1 - \frac{H}{\sqrt{R^2 + H^2}}\right) \quad \text{Eq. 11}$$

The calculated results of Ω(R,H,V) in the first case shown in Figure 4 agree very well with Ω_p within 0.008% error.

The formula of the second case given in ref. [2] is as follows

$$\Omega_D = \frac{2}{S^2}\int_S \Omega\left(\frac{R}{H}, \frac{S}{H}\right) r\,dr \quad \text{Eq. 12}$$

The calculated results of the second case using proposed Ω(R,H,V) instead of Ω(R/H,S/H) are given in Table 1. Simson's method for numerical integration with integration stepsize of 5×exp(-4) is used. Table 2 is given from ref. [2]. Results agree well within the error of 0.5% .

Conclusion

It is verified that the proposed method for the solid angle calculation will be useful when the incident angle of light is important such as optical fiber detector by comparison with other references. And it is expected that smaller integration stepsize produces more accurate results. The proposed method can be used to calculate not only the solid angle of optical fiber detector but also general circular solid angle.

Acknowledgements

This work was supported by the Korea Science Engineering Foundation (KOSEF) through the innovative Technology center for Radiation Safety (iTRS), Hanyang University.

References

[1] R. P. Gardner and A. Carnesale, Nucl. Instr. and Meth. 73 (1969) 228.
[2] R. P. Gardner and K. Verghese, Nucl. Instr. and Meth. 93 (1971) 163.
[3] C. Y. Yi and J. S. Jun, Rad. Prot. Dosi. 69, no. 2, p149 (1997)

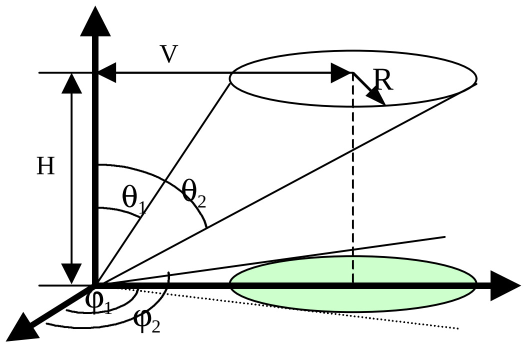

Figure 1 Notations used for calculation when R < V.

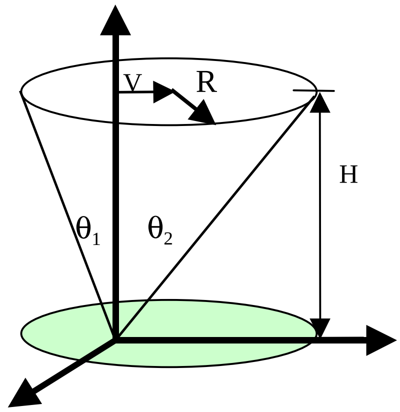

Figure 2 Notations for calculation when R ³ V.

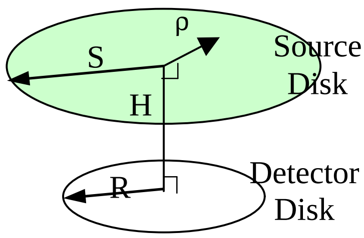

Figure 3 Notations used for calculation of average solid angle of a circular disk source subtended by a circular disk detector

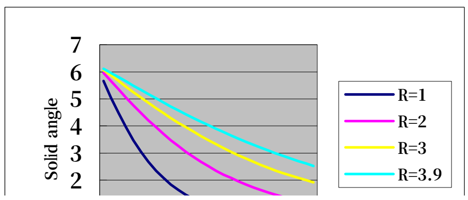

Figure 4 Graph of calculation of solid angle subtended by a circular disk at a point source lies on axis of disk. Radius of disk and distance are varied

Table 1 Average solid angle subtended by two coaxial disks values for various values of S/h and R/h by proposed method.

	S/H										
R/H	0.1	0.3	0.6	0.9	1.2	1.5	1.8	2.1	2.4	2.7	3
0.1	0.030794	0.029206	0.024775	0.019859	0.01567	0.012416	0.009961	0.008111	0.006704	0.005617	0.004766
0.2	0.120523	0.114617	0.09782	0.078817	0.062396	0.049537	0.039789	0.032424	0.02681	0.022472	0.019073
0.3	0.261879	0.250008	0.215387	0.174973	0.13926	0.110909	0.089248	0.072808	0.060244	0.050517	0.042889
0.4	0.444412	0.426276	0.371641	0.305237	0.244737	0.195775	0.157945	0.129049	0.106881	0.08968	0.076169
0.5	0.656433	0.632906	0.559241	0.465448	0.376696	0.303059	0.245322	0.200844	0.166549	0.139855	0.118847
0.6	0.886688	0.859341	0.770057	0.650562	0.532414	0.431357	0.350644	0.287791	0.239019	0.200907	0.170839
0.7	1.125463	1.096086	0.995942	0.85492	0.708616	0.578923	0.472985	0.389385	0.324002	0.272663	0.232037
0.8	1.365084	1.335331	1.229386	1.072581	0.901546	0.743662	0.611217	0.505008	0.421146	0.354914	0.302313
0.9	1.599942	1.57114	1.463951	1.297698	1.107082	0.923138	0.763993	0.633916	0.530029	0.447411	0.381513
1	1.826248	1.799344	1.694545	1.524914	1.320903	1.114589	0.929735	0.775228	0.650148	0.549855	0.469454
1.2	2.244972	2.223379	2.13021	1.968187	1.756416	1.521105	1.292621	1.090774	0.921642	0.783147	0.67068
1.4	2.61392	2.598143	2.520309	2.376974	2.177986	1.937478	1.68264	1.441375	1.229677	1.051289	0.90387
1.6	2.934663	2.92426	2.861552	2.740125	2.565149	2.339537	2.079925	1.813933	1.56638	1.349622	1.166214
1.8	3.21231	3.206519	3.1571	3.056413	2.908484	2.709534	2.464598	2.192897	1.921666	1.67203	1.454025
2	3.452838	3.450872	3.412518	3.329693	3.207096	3.038355	2.820634	2.561783	2.283257	2.010653	1.7625
2.2	3.661929	3.663093	3.63373	3.565605	3.464749	3.324556	3.138691	2.905985	2.637477	2.35574	2.08545
2.4	3.844569	3.848285	3.826158	3.769882	3.686904	3.571364	3.416279	3.215806	2.971151	2.695978	2.415096
2.6	4.004968	4.010771	3.994459	3.947661	3.879098	3.783907	3.655765	3.4875	3.274315	3.019683	2.742121
2.8	4.146621	4.15414	4.142516	4.103294	4.046276	3.967529	3.861791	3.722299	3.541998	3.31691	3.056326
3	4.272409	4.281349	4.273526	4.240381	4.192608	4.12705	4.039487	3.924193	3.774089	3.581635	3.348143

Table 2 Average solid angle subtended by two coaxial disks values for various values of S/h and R/h by Gardner

					S/h						
R/h	0.1	0.3	0.6	0.9	1.2	1.5	1.8	2.1	2.4	2.7	3
0.1	0.03095	0.02928	0.02476	0.01986	0.01567	0.01242	0.00997	0.00818	0.00671	0.00562	0.00477
0.2	0.12116	0.11481	0.09776	0.0788	0.06239	0.04954	0.0398	0.03243	0.02682	0.02248	0.01908
0.3	0.26328	0.28045	0.21526	0.17492	0.13924	0.11091	0.08925	0.07282	0.06025	3.05053	0.0429
0.4	0.4468	0.42708	0.37143	0.30515	0.2447	0.19577	0.15795	0.12906	0.10689	0.0897	0.07618
0.5	0.65997	0.63413	0.55891	0.46532	0.37664	0.30304	0.24532	0.20035	0.16656	0.13988	0.11887
0.6	0.89147	0.86103	0.7697	0.5039	0.53234	0.43134	0.35064	0.2978	0.23903	0.20094	0.17087
0.7	1.13154	1.09827	0.99552	0.85472	0.70853	0.5789	0.47299	0.3894	0.32402	0.27271	0.23208
0.8	1.37246	1.33801	1.2289	1.07237	0.90146	0.74364	0.61123	0.50503	0.42117	0.35498	0.30236
0.9	1.6086	1.57431	1.46338	1.39749	1.10699	0.92312	0.76401	0.63394	0.53006	0.44749	0.38158
1	1.83613	1.80299	1.69389	1.52472	1.32082	1.11458	0.92977	0.77527	0.6502	0.54996	0.46954
1.2	2.25712	2.22791	2.12937	1.96798	1.75641	1.52114	1.2927	1.09086	0.92173	0.78331	0.67081
1.4	2.62808	2.0346	2.5193	2.37672	2.17806	1.93761	1.68279	4.44153	1.22982	1.01554	0.90407
1.6	2.95056	2.93026	2.86038	2.73981	2.56524	2.3398	2.08017	1.81417	1.5666	1.34999	1.1665
1.8	3.22972	3.21311	3.15579	3.05603	2.90856	2.70986	2.46499	2.19324	1.92198	1.67254	1.45443
2	3.47156	3.45798	3.41108	3.32925	3.20716	3.03871	2.82114	2.56226	2328368	2.01134	1.76304
2.2	3.68179	3.67064	3.63819	3.56511	3.46478	3.32491	3.13924	2.90661	2362803	2.35664	2.08615
2.4	3.86541	3.85622	3.82453	3.76934	3.68692	3.57171	3.41685	3.2165	2.97185	2.69712	2.41599
2.6	4.02668	4.01905	3.99275	3.94708	3.87909	3.78425	3.65634	3.48823	3.27513	3.0211	2.74323
2.8	4.16911	4.16271	4.14074	4.10268	4.04625	3.96786	3.86237	3.72305	3.54286	3.31863	3.05769
3	4.29558	4.29018	4.27168	4.23974	4.19257	4.12738	4.04007	3.92495	3.77498	3.58357	3.34978